Micromotor-in-sponge platform for multi-cycle large-volume degradation of organic pollutants

Diana Vilela, Maria Guix, Jemish Parmar, Àngel Blanco-Blanes, Samuel Sánchez**

Dr. M. Guix, Dr. D. Vilela, Dr. J. Parmar, A. Blanco, Prof. S. Sánchez
Institute for Bioengineering of Catalonia (IBEC), The Barcelona Institute of Science and Technology (BIST). Baldiri-Reixac 10-12, 08028 Barcelona, Spain.
E-mail: mguix@ibecbarcelona.eu, ssanchez@ibecbarcelona.eu

Prof. S. Sánchez
Institució Catalana de Recerca i Estudis Avançats (ICREA). Passeig de Lluís Companys 23, 08010 Barcelona, Spain

Keywords: sponge, self-propelled micromotors, water treatment, organic pollutants

Abstract

The presence of organic pollutants in the environment is a global threat to human health and ecosystems due to their bioaccumulation and long-term persistence. We hereby present a micromotor-in-sponge concept that aims not only at pollutant removal, but towards an efficient in situ degradation by exploiting the synergy between the sponge hydrophobic nature and the rapid pollutant degradation promoted by the cobalt-ferrite (CFO) micromotors embedded at the sponge's core. Such platform allows the use of extremely low fuel concentration (0.13% H_2O_2), as well as its reusability and easy recovery. Moreover, we demonstrate an efficient multi-cycle pollutant degradation and treatment of large volumes (1L in 15min) by using multiple sponges. Such fast degradation process is due to the CFO bubble-propulsion motion mechanism, which induces both an enhanced fluid mixing within the sponge and an outward flow that allows a rapid fluid exchange. Also, we demonstrated the magnetic control of the system, guiding the sponge position during the degradation process. The micromotor-in-sponge configuration can be extrapolated to other catalytic micromotors, establishing an alternative platform for an easier implementation and recovery of micromotors in real environmental applications.

1. Introduction

The persistence of aromatic organic compounds generated from large-scale industrial activities is one of the most challenging environmental problems, causing adverse effects in humans and the environment.[1,2] Persistent organic pollutants (POPs), ranging from pesticides to industrial chemicals pose a serious health threat. Removal of POPs is key to establish efficient water remediation methods and ensure an efficient degradation to restrain bioaccumulation in the environment. Although promising degradation methods based on biodegradation[3,4] or photocatalytic[5] processes have been reported, advanced oxidative processes (AOPs) based on the generation of strong oxidizing agents (e.g. hydroxyl radicals, sulfate radicals) have been widely implemented in industry and they are one of the preferred methods.[6,7] Implementation of new technologies in well-known degradation processes have often lead to an enhanced degradation rate, as well as developing more versatile solutions for in-field applications. Engineered micro- and nanomotors have been exploited as active microcleaners for environmental purposes, showing an outstanding degradation performance due to the associated fluid mixing, as well as an efficient contaminant sensing.[8–11] During the last decade, these micro- and nanodevices have been designed with the aim of eliminating a wide range of pollutants through different physical and chemical processes such as physisorption[12–20] and biological-based capture,[21] degradation,[22–38] and cell lysis[39–42] or combination of some of them.[17,43,44] Among them, degradation processes which include catalysis,[23,24,30,45,46] photocatalysis[25,26,36–38] and enzymatic catalysis,[27–29] are the most widely used mechanisms for the removal of organic pollutants. Particularly, Fenton-like reactions have been explored as efficient decontaminating processes of AOPs in both bubble propelled platinum[23,45] or MnO_2[17,43,47] microtubes and cobalt ferrite microparticles (CFO),[48] demonstrating exceptional degradation rates. Although some of the nano/micromotors design up to date avoided the use of costly fabrications processes[48–50] aiming for mass production to permit the technology transfer of such active microcleaners in real applications, there is still one main concern: how to deploy them safely while keeping

high performance to reuse and recover them in order to ensure a green and sustainable degradation process. In our work, we aim to cover this gap in the nano/micromotors community, demonstrating a universal solution for an easy recovery and multi-cycle degradation process. This is possible by confining the micromotors in a sponge structure that presents an internal spherical cavity that ensure their free motion. Additionally, the absorbent properties of the sponge are also exploited, resulting in an (i) untethered degradation platform, with (ii) high degradation efficiency arising from the active embedded microcleaners, and permitting (iii) easy micromotors recovery as well as (iv) the reusability of the micromotor-in-sponge system, reducing the costs of the overall degradation process.

The development of sponges for environmental remediation have generally been associated to the absorption of certain pollutants for recycling and/or recovery purposes, ranging from organic pollutants to oil spill.[51] They have been applied both as sponge membranes in bioreactors [52,53] or stand-alone absorption platforms, where both their surface topography[54] or chemical composition [55–58] were studied, as well as exploring alternative composites for faster magnetic separation[59] or precise motion control by applying external magnetic fields.[60] However, it is important to note that for the examples previously mentioned, there was only a pollutant separation for recovery purposes, but no degradation process was undertaken either during the collection process or afterwards. Towards that aim, different catalyst have been included within the sponge network for chemical[61,62] or light-induced[63,64] degradation purposes, as well as varying the sponge wettability.[65]

Here, we report a new concept of a degradation platform based on a sponge loaded with cobalt-ferrite (CFO) micromotors, which exploits both the advantages of the sponge porous polyurethane-based material to capture pollutants and the in-situ degradation of such pollutants by the catalytic micromotors. CFO micromotors are self-propelled heterogeneous Fenton-like catalysts whose activation is triggered in presence of hydrogen peroxide. The

solvothermal fabrication method used allows high production rates of CFO nanoparticles with the size under 100 μm.[48] CFO micromotors are located in spherical cavities inside the sponge's structure and their characteristic bubble-recoil motion mechanism not only provides an enhanced in situ pollutant degradation under extremely low fuel concentration (0.13%) when compared to previous micromotor-based degradation approaches,[17,23,66] but also an increased intra-sponge pressure that promotes fluid pumping, useful to improve mixing and fluid exchange in wastewater degradation processes. Therefore, the combination of the sponge and CFO micromotors results in a synergistic concept with high performance for organic pollutant degradation. This untethered degradation presents an integrated solution, allowing pollutant attraction, enhanced degradation, and improved solution exchange in a single system which can be reused and applied in large volumes. Apart from demonstrating an efficient degradation in large volumes and platform reusability, the micromotor's confinement in the sponge allows a facile recovery for multi-cycle degradation, providing a new insight for the design of future micromotor-based platforms for real environmental applications, as the micromotor-in-sponge concept could be extended to other catalytic micromotors.

Figure 1A shows a schematic illustration of the sponge, with a characteristic mushroom-like shape that facilitates its floatability during the degradation process, and the inner cavities, where CFO micromotors are confined. CFO catalytic micromotors are activated in presence of hydrogen peroxide (H_2O_2), promoting an enhanced oxidative of removal POPs or antibiotics by Fenton-Like reaction and due to their bubble- propelled active motion (**Figure 1**B).[48] In this specific case, CFO are confined in the sponge, allowing an effective micromotors activation at ultra-low fuel concentration by directly soaking H_2O_2 in the sponge before the degradation process to ensure a fuel pre-concentration at the sponge inner cavities where catalytic micromotors are (volume loaded/sponge: 6 mL). Additionally, the active mixing at the inner core of the sponge not only promotes an accelerated degradation

in the cavities, but also an active pumping arising from the overpressure associated to bubble generation. This effect is observed in **Figure 1**C, where two-phase system is shown just under the sponge in absence of stirring, consequence of the fluid flows generated within the sponge and which promotes a fluid exchange (**Movie 1**, SI), allowing large volume degradation in a short time frame.

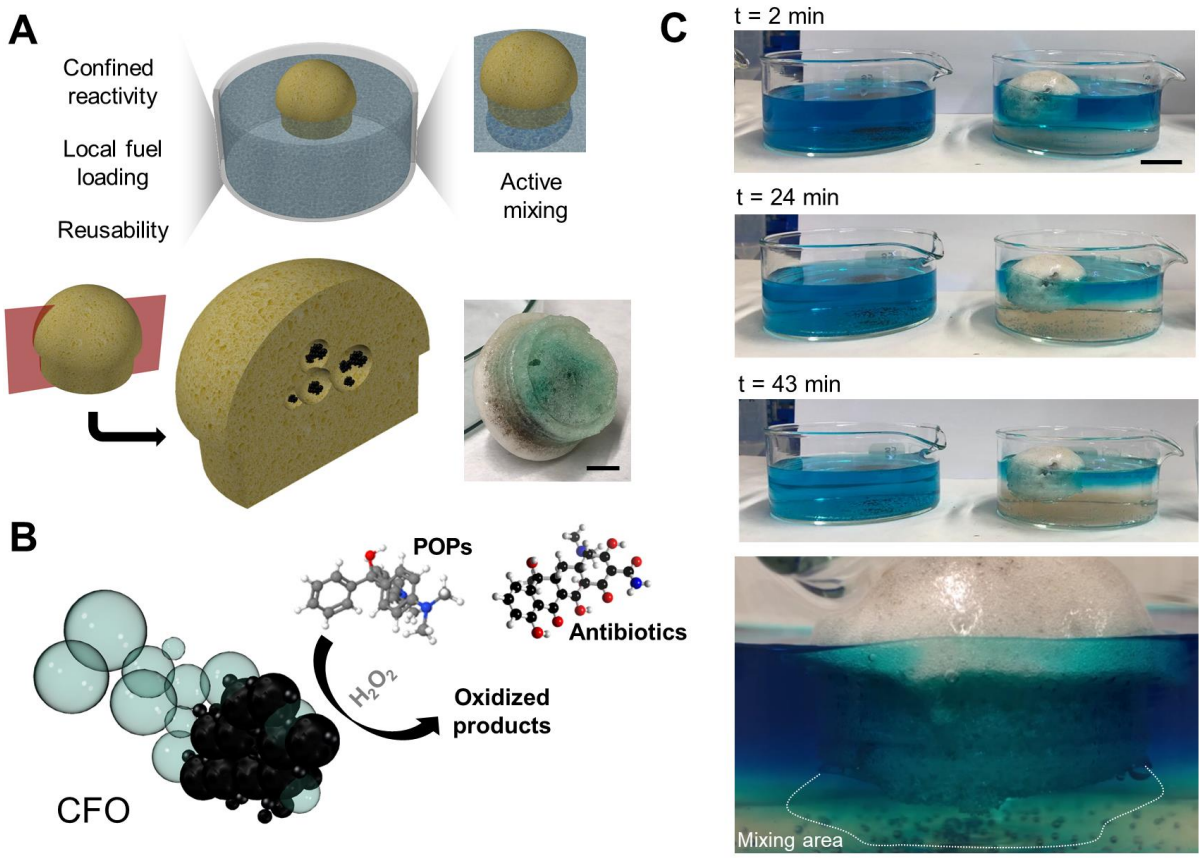

Figure 1. Structure and degradation behavior of sponge loaded with cobalt-ferrite (CFO). A) Schematic of the degradation setup (above) and cross-section of a CFO-sponge with inner cavities loaded with CFO catalytic micromotors (below), optical image a CFO-sponge after a degradation process. B) Schematic of organic pollutants degradation by CFO catalytic micromotors. C) Degradation over time (2, 24, 43 min) of malachite green by using CFO-sponges; right: control assay at 0.33% (v/v) H_2O_2, left: CFO-sponge degradation loaded with 0.33% (v/v) H_2O_2 under no stirring. Below, side view photo of a CFO-sponge during the

degradation process, depicting the mixing area due to the overpressure created by the bubble-recoil micromotors embedded within the sponge structure (**Movie 2**). Scale bar, 1cm.

The main characteristic of the hereby presented sponge configuration, are the spherical inner cavities loaded with CFO micromotors, which is achieved by embedding the CFO in millimeter scale alginate capsules. While the porous morphology is ensured by a good mixing of the two polymeric components (more details in experimental section), the mushroom-like shape from the sponge is achieved by the two-layer deposition onto a rigid plastic mold with a circular shape (**Figure 2**A and S1). After the first deposition, the CFO-loaded alginate particles were in the very middle before proceeding to the second-layer deposition. This is key to not only include the micromotors inside the sponge, but also to ensure the presence of cavities that will allow its motion and enhanced fluid mixing during the degradation process. After 30 min, when the polyurethane porous material is well-polymerized, the sponge is released from the rigid mold. Afterwards we ensure the dissolution and further cavity creation inside the sponge by dissolving the alginate with sodium citrate. The morphology and composition of the CFO micromotors were first confirmed through Scanning Electron Microscopy (SEM), Transmission Electron Microscopy (TEM) and Energy-dispersive X-ray spectroscopy (EDX) (Figure S2). Then, the corresponding characterization studies of the micromotor-in-sponge platform by SEM demonstrated the presence of CFO at the inner sponge cavities (**Figure 2**B and S3). Also, the hydrophobic nature of the polyurethane-based sponge was studied by evaluating contact angle (**Figure 2**C), observing and initial hydrophobic behavior that changes over time, leading to a more hydrophilic behavior after a few minutes, presenting an initial contact angle of 101º and a contact of 76º after 3 minutes. Therefore, we can relate such properties to the organic pollutant attraction/absorption into the sponge observed during the degradation process (hydrophobic properties), but also the high degradation efficiency due to the enhanced fluid exchange in the water-based solution

(hydrophilic properties). Finally, the magnetic properties from the CFO micromotors also allowed us to perform an external control over the position of the micromotor-in-sponge platform by using a permanent magnet, as demonstrated in Figure 2D.

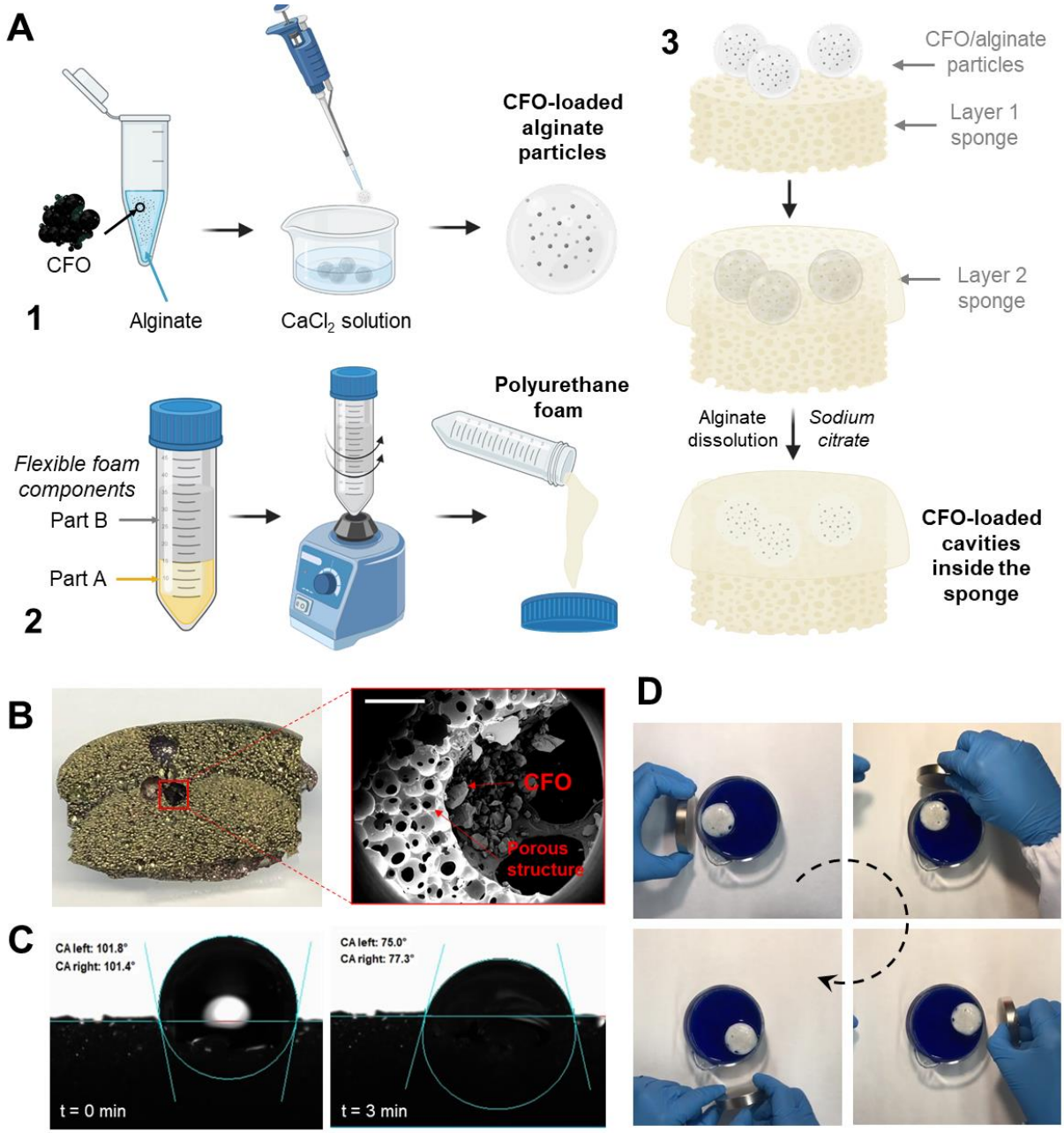

Figure 2. CFO-sponge fabrication and characterization. A) Schematic of the CFO-sponge fabrication process. Created with BioRender.com. B) Optical image of a gold-sputtered longitudinal-section of a CFO-sponge, with the corresponding SEM image from the cavity with the CFO catalytic micromotors. C) Contact angle from the smooth outer surface of the CFO sponge. D) Direction control of CFO-sponges by using neodymium magnet.

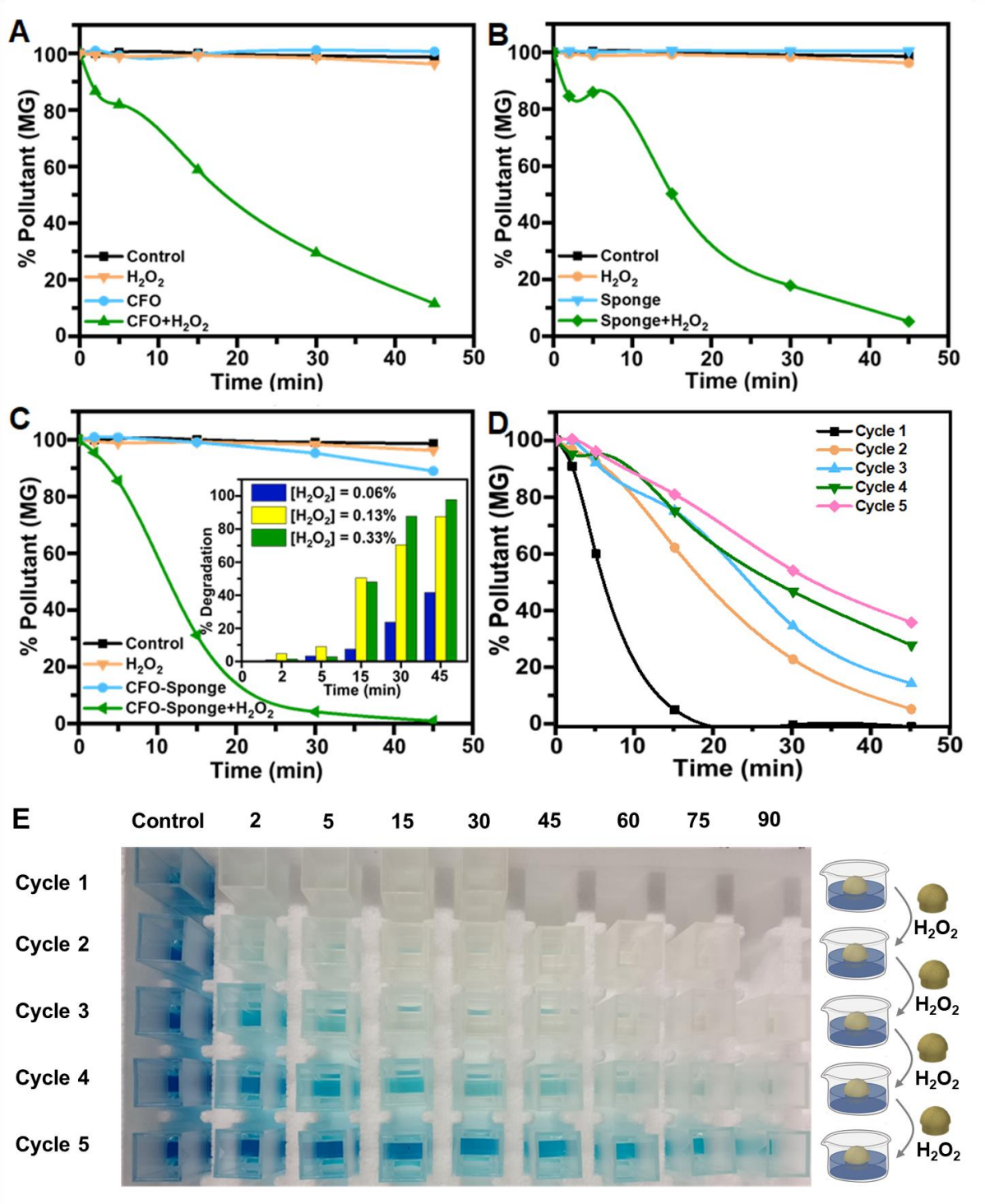

Figure 3. Removal of malachite green (MG) in water over time using CFO-sponges: Kinetics of catalytic degradation of MG (A) using CFO micromotors, (B) a sponge and (C) a CFO-sponge (Inset: Catalytic degradation of MG using CFO-sponges at 0.06, 0.13 and 0.33% (v/v) H_2O_2 concentrations, respectively). (D) Reusability performance of CFO-sponges in

consecutive MG degradations during five cycles. (E) Optical snapshot from the MG contaminated solutions over time during the five cycles of reusability (Experimental conditions: 0.33% (v/v) of H_2O_2, 50 µg/mL of MG and total volume of MG solution = 100 mL).

To prove the degradation performance of CFO-sponges as efficient tools for the removal of organic pollutants such as POPs, malachite green (MG) has been selected as model pollutant. First, we evaluated MG removal capacity of CFO-sponges as well as each of their parts individually (Figure 3 A-C). For this purpose, we employed systematically a CFO-sponge and a concentration of 0.33% (v/v) of H_2O_2 in all experiments for the degradation of 100 mL of 50 µg/mL of MG. In parallel to this assay, the number of motors contained within the sponge as well as the sponge itself were evaluated for MG degradation under the same conditions. As expected, we observed that CFO-sponges showed the best degradation rate, about 90 % after 20 minutes of treatment, (Figure 3C) in comparison with the degradation rates of 53% obtained for CFO micromotors (Figure 3A) and 68 % for sponges (Figure 3B), respectively, at the same time. In previous reports,[45] by using Fe/Pt microcleaners only 75% degradation for a 3ml MG solution at the same concentration is achieved after 60 min in presence of 5% H_2O_2 solution and surfactant (SDS, 0.5% w/v). In contrast, the micromotor-in-sponge platform provides a faster degradation rate in larger volumes, also avoiding the use of any surfactant and allowing an easier recovery of the micromotors after the degradation process. These results are supported by the multiple functionalities that CFO-sponges present in a unique device enabling the absorption and degradation of organic molecules as well as their active diffusion in the contaminated solution by an intrinsic mixing effect caused by the bubble generation and release from the inner cavities of these devices (**Movie 1**, SI).

Regarding the high efficacy that CFO-sponges showed for the pollutant degradation and to reduce costs and contamination, we studied the effect of decreasing the H_2O_2 concentration. To this end, we selected three H_2O_2 concentrations (0.33%, 0.13% and 0.06% (v/v)). As

displayed in the inset of Figure 3C, degradation rate decreases as peroxide concentration decreases and reaching a maximum at 0.33% (v/v). This fact indicates that degradation is originated from CFO oxidative reaction, generating a greater number of hydroxyl radicals and consequently, a faster degradation of organic molecules.[48] Thus, 0.33% (v/v) was selected as optimized concentrations for further experiments.

A common challenge in the implementation of catalytic micromotors for environmental purposes is how to recover them after the pollutant degradation process. In the proposed configuration the solution by using the sponge configuration is assessed, demonstrating an easy micromotors' recovery and reusability of the micromotor-in-sponge system in consecutive degradation cycles in a large volume. Therefore, reusability studies of CFO-sponges were done in five consecutive cycles through short-term experiments varying time intervals (**Figure 3**D and E). This assay was carried out using one CFO-sponge under the conditions set in the tests previously introduced and continuously changing polluted water after the end of the 45 minutes of a degradation cycle. As observed in Figure 3D and 3E, despite the removal efficiency decreases slightly with each reusability cycle, CFO-sponges can be reused more than 3 times losing less than 20% of decontamination capacity and up to 5 times without losing more than 40%.

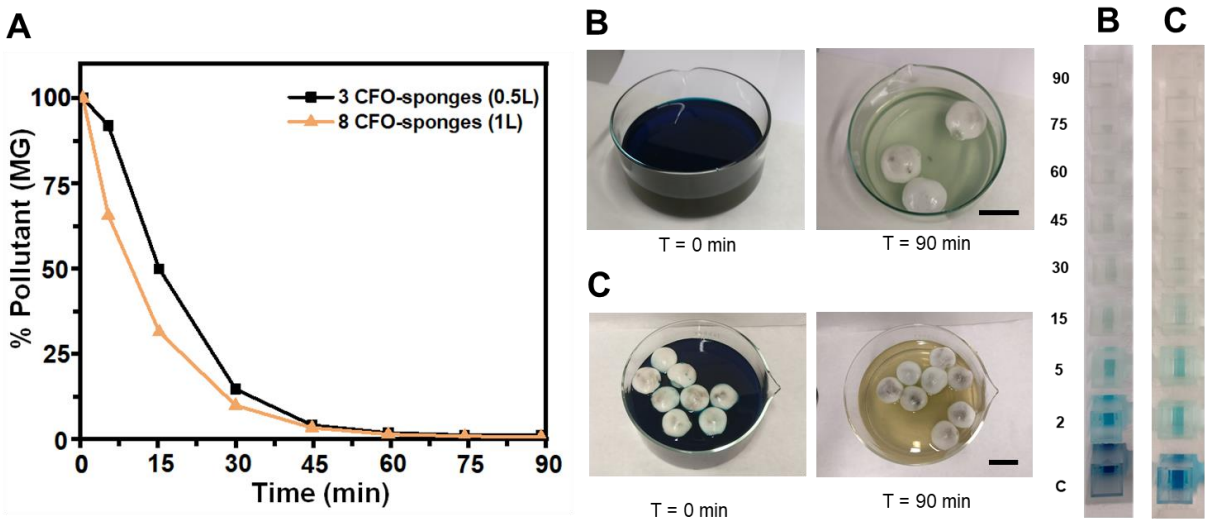

Figure 4. Removal of malachite green (MG) in water over time using several CFO-sponges: (A) Kinetics of catalytic degradation of MG using 3 and 8 CFO-sponges loaded with 5% (v/v) H_2O_2 in big volumes of contaminated solutions (0.5 and 1L, respectively). Degradation of MG and optical snapshot from the MG contaminated solutions over time using 3 (B) and 8 (C) CFO-sponges, respectively, after 90 min (Experimental conditions: 0.20% (v/v) and 0.26% (v/v) of H_2O_2 for 3 and 8 CFO-sponges, respectively, 50 µg/mL of MG solution). Scale bar, 4 cm.

Another challenge that needs to be addressed before the implementation of the current technology in real scenarios is its scalability, considering both the cost of the materials used and consequent mass production, and the ability to degrade large volumes. In our case, we selected CFO micromotors as the catalytic source of the micromotor-loaded sponges, using inexpensive materials and following a synthesis that can easily be mass produced, as well as not requiring any surfactants during the micromotors activation, in contrast to the majority of micromotor-based degradation processes.[48] On the other hand, the materials related to the sponge fabrication are also inexpensive and easy to produce in large quantities, showing the desired absorption capabilities,[67] as well as allowing the creation of an inner spherical cavity where micromotors are confined but able to move autonomously, at the same that they interact with the surrounding solution due to the porous nature from the sponge. To demonstrate the potential scalability of the micromotor-in-sponge platform, we evaluated CFO-sponges for the MG degradation in big volumes, such as 0.5 and 1L (**Figure 4**). This assay was carried out using the experimental conditions detailed in Figure 3 but increasing the volumes of MG solution, as well as the total number of CFO-sponges employed. As it is shown in Figure 4, three and eight CFO-sponges were able to totally degrade 0.5 and 1 L solutions of MG in 45 minutes, respectively, thus demonstrating the scalability of micromotors-loaded sponges.

In conclusion, we prepared a micromotor-loaded sponge platform, where active CFO micromotors are confined in the spherical cavity at the sponge's core. The hydrophobic nature of the sponge aids pollutant attraction, while the catalytic micromotors' bubble-propelled motion mechanism allows an enhanced fluid mixing within the sponge's cavity, and a rapid fluid exchange with the surrounding solution. Altogether, these factors result in an enhanced degradation process that permits water treatment in large volumes. Additionally, the untethered nature of the current platform allows not only an easy nanomotors recovery, but we demonstrated its reusability by efficiently performing five consecutive degradation cycles. The magnetic nature of the embedded CFO micromotors allows an on-demand control of its location during the degradation process. The key features of the micromotor-in-sponge platform rely on its versatility, allowing an easy integration of other bubble-propelled micromotors at the inner cavity, and opening the door to the real implementation of micromotor-based degradation methods in large-scale environmental systems. Also, by properly chemically functionalizing the sponge,[55,64,65] the current system could be envisioned for selective pollutant degradation and the micromotor-in-sponge lifetime could be extended, resulting in a more profitable wastewater treatment platform.

Experimental Section

Materials: Self skinning flexible polyurethane foam (410-035, Tiranti, Ltd, UK). Cobalt acetate (CoAc, 403024), iron(III)chloride hexahydrate ($FeCl_3 \cdot 6H_2O$, F2877), sodium acetate anhydrous (NaAc, S8750), ethylene glycol (324558), sodium acetate (NaAc, S8750), malachite green oxalate salt (M9015), calcium chloride dihydrate ($CaCl_2 \cdot 2H_2O$, C3306), sodium alginate (W201502), sodium citrate dihydrate (W302600), and hydrogen peroxide (95294), were purchased from Sigma-Aldrich. Polyethylene glycol (PEG 200,Alfa Aesar B21918). Isopropanol (Panreac 211090).

Cobalt ferrite micromotors synthesis: Cobalt ferrite (CFO) micromotors were fabricated from cobalt ferrite nanoparticles. Cobalt ferrite nanoparticles were synthesized by solvothermal method using CoAc and $FeCl_3 \cdot 6H_2O$, as the precursors. First, 0.92 g CoAc and 1 g $FeCl_3 \cdot 6H_2O$ were dissolved in 30 mL of ethylene glycol. Then, 2.78 g of NaAc and 1 mL of PEG 200 as the stabilizer were added to the previous mix. The prepared solution was transferred into 50 mL Teflon lined hydrothermal autoclave and heated to 170ºC for 15 h. After the reaction was completed, the reactor was cool down to room temperature and then the content was transferred into a beaker. The nanoparticle suspension obtained was washed multiple times with isopropanol to remove ethylene glycol and unreacted precursor molecules. Then, the resulting suspension was dried using an oven at 80ºC for 15 h. The drying process induces the aggregation of the cobalt ferrite nanoparticles into few hundred-micrometers sizes of microparticles. These microparticles were manually grounded and sieved to obtain CFO micromotors with the size under 100 µm.

Sponge fabrication: The sponge configuration is based on a porous polyurethane-based platform with a mushroom-like shape that contains inner cavities where the CFO micromotors are found. To obtain the right porosity, the two components from the commercial foam kit were mixed at a ratio of 2:1, component A: component B. It is key to firstly mixed them with and spatula and then at the vortex stirrer at 2500 rpm, till the mixture start expanding spontaneously. At this stage, it poured the first layer on a plastic cap (Figure 2A). To ensure the creation of the cavities and embedment of the CFO inside the sponge, alginate particles previously loaded with the CFO at the interface of the first and second layer of foam. Such alginate particles were obtained by pouring drop by drop 1 mL alginate (2%) with CFO micromotors (53 mg/mL) into a $CaCl_2$ bath in constant stirring. The resulting particles had a diameter of about 3 mm and were washed with milliQ water before their integration in the sponge. After being deposited on the first layer of foam, a second layer of foam is casted onto

them. After 30 minutes, the whole construct can be detached from the cap, and the lower thin layer of polymer is cut to ensure improved absorption and fluid mixing during the degradation process. The sponge is soaked with sodium citrate at 0.2M for 10 minutes to dissolve alginate, resulting in cavities that permit a free motion from the CFO micromotors while achieving their confinement within the sponge scaffold.

Characterization on CFO morphology and composition: CFO micromotors morphology was evaluated by using scanning electron microscopy (SEM) microscopy (FEI NOVA NanoSEM 230 at 5 kV) and Transmission electron microscopy (TEM), where Energy-dispersive X-ray spectroscopy (EDX) was also performed (JEOL 1010).

Characterization on Structural Features of the Sponge: To evaluate the morphology at the micro- and mesoscale, to both observe the porous structure of the sponge and the cavities where CFO micromotors were confined, we performed a longitudinal section of the sponge and sputtered 15nm gold layer on it to further evaluate it by SEM. SEM images at different magnifications were acquired by using a FEI NOVA NanoSEM 230 at 5 kV.

Sponge wettability characterization: Contact angle was measured using an optical contact angle measurement (OCA15Pro, DataPhysics Instruments GmbH, Germany).

Measurement of pollutant degradation: Malachite green (MG) and tetracycline (TC, sigma T7660) were selected as target POPs molecules. MG was selected as model POPs to study and optimize the degradation approach of the CFO-sponges. For the degradation of this organic chemical, CFO-sponge loaded with hydrogen peroxide (5% v/v) were placed in a glass beaker containing total 100 mL of polluted water. First, we studied the degradation performance of CFO-sponges in comparison with equivalent quantity of free CFO-micromotors and a sponge without micromotors inside. Then, to achieve the optimized H_2O_2 concentration for MG degradation using CFO-sponges, we evaluated three concentrations

H_2O_2. This involved the loading of CFO-sponges with H_2O_2, 5% (v/v), 2% (v/v) and 1% (v/v), which are equivalent to 0.33% (v/v), 0. 13% (v/v), and 0.06% (v/v), respectively, as final concentrations in solution. Reusability experiments were carried out following the same conditions of the first MG decontamination. After each cycle, the CFO-sponges were recovered washed with water and reloaded with 5% (v/v) H_2O_2 to start a new degradation cycle. This operation was repeated up to five times. Finally, scalability was proved in 0.5L and 1L of MG solution using three and eight CFO-sponges, respectively, loaded with 5% (v/v) H_2O_2.

Supporting Information

Supporting Information is available from the Wiley Online Library or from the author.

Acknowledgements

D.V. and M.G. contributed equally to this work. M.G. thanks MINECO for the Juan de la Cierva fellowship (IJCI2016-30451), the Beatriu de Pinós Programme (2018-BP-00305) and the Ministry of Business and Knowledge of the Government of Catalonia. D. V. thanks . acknowledges financial support by the European Commission under a Horizon 2020 Marie Skłodowska-Curie Action COFUND scheme (grant agreement no. 712754) and by the Severo Ochoa program of the Spanish Ministry of Economy and Competitiveness (grant no. SEV2014-0425). S.S. acknowledges the CERCA program by the Generalitat de Catalunya, the Secretaria d'Universitats i Recerca del Departament d'Empresa I Coneixement de la Generalitat de Catalunya through the project 2017 SGR 1148 and Ministerio de Ciencia, Innovación y Universidades (MCIU) / Agencia Estatal de Investigación (AEI) / Fondo Europeo de Desarrollo Regional (FEDER, UE) through the project RTI2018-098164-B-I00. This project was also partially funded by Agencia Estatal de Investigación (CEX2018-000789-S). All the authors acknowledge MicroFabSpace and Microscopy Characterization Facility, Unit 7 of ICTS "NANBIOSIS" from CIBER-BBN at IBEC for their support regarding the sponge morphological characterization.

Received: ((will be filled in by the editorial staff))
Revised: ((will be filled in by the editorial staff))
Published online: ((will be filled in by the editorial staff))

References

[1] R. Weber, A. Watson, M. Forter, F. Oliaei, *Waste Manag. Res. J. a Sustain. Circ. Econ.* **2011**, *29*, 107.

[2] "European Union (Persistent Organic Pollutants) Regulations 2020," can be found under https://ec.europa.eu/environment/chemicals/international_conventions/index_en.htm, **n.d.**

[3] S. Bajaj, D. K. Singh, *Int. Biodeterior. Biodegradation* **2015**, *100*, 98.

[4] N. Gaur, K. Narasimhulu, P. Y, *J. Clean. Prod.* **2018**, *198*, 1602.

[5] T. T. Nguyen, H. H. Ngo, W. Guo, A. Johnston, A. Listowski, *Bioresour. Technol.* **2010**, *101*, 1416.

[6] J. O. Tijani, O. O. Fatoba, G. Madzivire, L. F. Petrik, *Water, Air, Soil Pollut.* **2014**, *225*, 2102.

[7] M. A. Oturan, *Environ. Sci. Pollut. Res.* **2014**, *21*, 8333.

[8] L. Soler, S. Sánchez, *Nanoscale* **2014**, *6*, 7175.

[9] W. Gao, J. Wang, *ACS Nano* **2014**, *8*, 3170.

[10] J. Parmar, D. Vilela, K. Villa, J. Wang, S. Sánchez, *J. Am. Chem. Soc.* **2018**, *140*, 9317.

[11] B. Jurado-Sánchez, J. Wang, *Environ. Sci. Nano* **2018**, *5*, 1530.

[12] D. Vilela, J. Parmar, Y. Zeng, Y. Zhao, S. Sánchez, *Nano Lett.* **2016**, *16*, 2860.

[13] D. Vilela, A. C. Hortelao, R. Balderas-Xicohténcatl, M. Hirscher, K. Hahn, X. Ma, S. Sánchez, *Nanoscale* **2017**, *9*, 13990.

[14] H. Wang, M. G. Potroz, J. A. Jackman, B. Khezri, T. Marić, N.-J. Cho, M. Pumera, *Adv. Funct. Mater.* **2017**, *27*, 1702338.

[15] B. Jurado-Sánchez, S. Sattayasamitsathit, W. Gao, L. Santos, Y. Fedorak, V. V. Singh, J. Orozco, M. Galarnyk, J. Wang, *Small* **2015**, *11*, 499.

[16] T. Hou, S. Yu, M. Zhou, M. Wu, J. Liu, X. Zheng, J. Li, J. Wang, X. Wang, *Nanoscale* **2020**, *12*, 5227.

[17] X. Ding, Y. Liu, X. Chen, W. Liu, J. Li, *Chem. – An Asian J.* **2021**, asia. 202100448.

[18] M. Guix, J. Orozco, M. García, W. Gao, S. Sattayasamitsathit, A. Merkoçi, A. Escarpa,

J. Wang, *ACS Nano* **2012**, *6*, 4445.

[19] F. Mou, D. Pan, C. Chen, Y. Gao, L. Xu, J. Guan, *Adv. Funct. Mater.* **2015**, *25*, 6173.

[20] V. V. Singh, A. Martin, K. Kaufmann, S. D. S. de Oliveira, J. Wang, *Chem. Mater.* **2015**, *27*, 8162.

[21] S. Campuzano, J. Orozco, D. Kagan, M. Guix, W. Gao, S. Sattayasamitsathit, J. C. Claussen, A. Merkoçi, J. Wang, *Nano Lett.* **2011**, *12*, 396.

[22] J. Parmar, D. Vilela, S. Sanchez, *Eur. Phys. J. Spec. Top.* **2016**, *225*, 2255.

[23] L. Soler, V. Magdanz, V. M. Fomin, S. Sanchez, O. G. Schmidt, *ACS Nano* **2013**, *7*, 9611.

[24] L. Chen, H. Yuan, S. Chen, C. Zheng, X. Wu, Z. Li, C. Liang, P. Dai, Q. Wang, X. Ma, X. Yan, *ACS Appl. Mater. Interfaces* **2021**, *13*, 31226.

[25] A. M. Pourrahimi, K. Villa, C. L. M. Palenzuela, Y. Ying, Z. Sofer, M. Pumera, *Adv. Funct. Mater.* **2019**, *29*, 1808678.

[26] L. Wang, A. Kaeppler, D. Fischer, J. Simmchen, *ACS Appl. Mater. Interfaces* **2019**, *11*, 32937.

[27] S. Sattayasamitsathit, K. Kaufmann, M. Galarnyk, R. Vazquez-Duhalt, J. Wang, *RSC Adv.* **2014**, *4*, 27565.

[28] J. Orozco, D. Vilela, G. Valdés-Ramírez, Y. Fedorak, A. Escarpa, R. Vazquez-Duhalt, J. Wang, *Chem. – A Eur. J.* **2014**, *20*, 2866.

[29] M. Uygun, V. de la Asunción-Nadal, S. Evli, D. A. Uygun, B. Jurado-Sánchez, A. Escarpa, *Appl. Mater. Today* **2021**, *23*, 101045.

[30] O. M. Wani, M. Safdar, N. Kinnunen, J. Jänis, *Chem. – A Eur. J.* **2016**, *22*, 1244.

[31] Y. Zhang, H. Li, M. Chen, X. Fang, P. Pang, H. Wang, Z. Wu, W. Yang, *Sensors Actuators, B Chem.* **2017**, *249*, 431.

[32] L. Wang, H. Zhu, Y. Shi, Y. Ge, X. Feng, R. Liu, Y. Li, Y. Ma, L. Wang, *Nanoscale* **2018**, *10*, 11384.

[33] F. Mushtaq, A. Asani, M. Hoop, X.-Z. Chen, D. Ahmed, B. J. Nelson, S. Pané, *Adv. Funct. Mater.* **2016**, *26*, 6995.

[34] J. Wang, R. Dong, Q. Yang, H. Wu, Z. Bi, Q. Liang, Q. Wang, C. Wang, Y. Mei, Y. Cai, *Nanoscale* **2019**, *11*, 16592.

[35] J. Tong, D. Wang, D. Wang, F. Xu, R. Duan, D. Zhang, J. Fan, B. Dong, *Langmuir* **2019**, *36*, 6930.

[36] L. Chen, M.-J. Zhang, S.-Y. Zhang, L. Shi, Y.-M. Yang, Z. Liu, X.-J. Ju, R. Xie, W. Wang, L.-Y. Chu, *ACS Appl. Mater. Interfaces* **2020**, *12*, 35120.

[37] Y. Liu, J. Li, J. Li, X. Yan, F. Wang, W. Yang, D. H. L. Ng, J. Yang, *J. Clean. Prod.* **2020**, *252*, 119573.

[38] E. Ma, K. Wang, Z. Hu, H. Wang, *J. Colloid Interface Sci.* **2021**, *603*, 685.

[39] J. A. M. Delezuk, D. E. Ramírez-Herrera, B. E.-F. de Ávila, J. Wang, *Nanoscale* **2017**, *9*, 2195.

[40] D. Vilela, M. M. Stanton, J. Parmar, S. Sánchez, *ACS Appl. Mater. Interfaces* **2017**, *9*, 22093.

[41] M. Hoop, Y. Shen, X.-Z. Chen, F. Mushtaq, L. M. Iuliano, M. S. Sakar, A. Petruska, M. J. Loessner, B. J. Nelson, S. Pané, *Adv. Funct. Mater.* **2016**, *26*, 1063.

[42] H. Xin, N. Zhao, Y. Wang, X. Zhao, T. Pan, Y. Shi, B. Li, *Nano Lett.* **2020**, *20*, 7177.

[43] K. Villa, J. Parmar, D. Vilela, S. Sánchez, *ACS Appl. Mater. Interfaces* **2018**, *10*, 20478.

[44] X. He, Y. K. Bahk, J. Wang, *Chemosphere* **2017**, *184*, 601.

[45] J. Parmar, D. Vilela, E. Pellicer, D. Esqué-de los Ojos, J. Sort, S. Sánchez, *Adv. Funct. Mater.* **2016**, *26*, 4152.

[46] M. Bayraktaroğlu, B. Jurado-Sánchez, M. Uygun, *J. Hazard. Mater.* **2021**, *418*, 126268.

[47] R. Maria-Hormigos, M. Pacheco, B. Jurado-Sánchez, A. Escarpa, *Environ. Sci. Nano* **2018**, *5*, 2993.

[48] J. Parmar, K. Villa, D. Vilela, S. Sánchez, *Appl. Mater. Today* **2017**, *9*, 605.

[49] S. Hermanová, M. Pumera, *Nanoscale* **2018**, *10*, 7332.

[50] J. Li, M. Pumera, *Chem. Soc. Rev.* **2021**, *50*, 2794.

[51] T. D. Minh, M. C. Ncibi, V. Srivastava, B. Doshi, M. Sillanpää, *Chemosphere* **2021**, *271*, 129516.

[52] T.-T. Nguyen, X.-T. Bui, V.-P. Luu, P.-D. Nguyen, W. Guo, H.-H. Ngo, *Bioresour. Technol.* **2017**, *240*, 42.

[53] A. M. Almusawy, R. H. Al-Anbari, Q. F. Alsalhy, A. I. Al-Najar, *Membranes (Basel).* **2020**, *10*, 433.

[54] Y. Cui, Y. Wang, Z. Shao, A. Mao, W. Gao, H. Bai, *Adv. Mater.* **2020**, *32*, 1.

[55] B. Ge, Z. Zhang, X. Zhu, X. Men, X. Zhou, *Colloids Surfaces A Physicochem. Eng. Asp.* **2014**, *457*, 397.

[56] Z. Wan, D. Li, Y. Jiao, X. Ouyang, L. Chang, X. Wang, *Appl. Mater. Today* **2017**, *9*, 551.

[57] N. Gissawong, S. Mukdasai, S. Boonchiangma, S. Sansuk, S. Srijaranai, *Chemosphere* **2020**, *260*, 127590.

[58] Y. Hwang, M. S. Bin Ibrahim, J. Deng, J. A. Jackman, N. Cho, *Adv. Funct. Mater.* **2021**, *31*, 2101091.

[59] B. Yu, X. Zhang, J. Xie, R. Wu, X. Liu, H. Li, F. Chen, H. Yang, Z. Ming, S. T. Yang, *Appl. Surf. Sci.* **2015**, *351*, 765.

[60] W. Ma, H. Wang, *Appl. Mater. Today* **2019**, *15*, 263.

[61] L. Zhu, J. Ji, J. Liu, S. Mine, M. Matsuoka, J. Zhang, M. Xing, *Angew. Chemie - Int. Ed.* **2020**, *59*, 13968.

[62] J. Cao, Y. Wang, D. Wang, R. Sun, M. Guo, S. Feng, *Macromol. Rapid Commun.* **2021**, *42*, 1.

[63] R. Hickman, E. Walker, S. Chowdhury, *J. Water Process Eng.* **2018**, *24*, 74.

[64] S. Sui, H. Quan, Y. Hu, M. Hou, S. Guo, *J. Colloid Interface Sci.* **2021**, *589*, 275.

[65] X. Xu, M. Li, X. Li, L. Zhang, *J. Ind. Eng. Chem.* **2020**, *92*, 278.

[66] J. Wang, R. Dong, Q. Yang, H. Wu, Z. Bi, Q. Liang, Q. Wang, C. Wang, Y. Mei, Y. Cai, *Nanoscale* **2019**, *11*, 16592.

[67] A. Kausar, *Polym. Plast. Technol. Eng.* **2018**, *57*, 346.

The micromotor-in-sponge platform provides an efficient in situ degradation due to the synergy of the sponge hydrophobic nature and the rapid pollutant degradation by motile cobalt-ferrite (CFO) micromotors embedded at the sponge' core. Its environmental degradation performance is demonstrated in large volumes by using extremely low fuel concentration, as well as its reusability and easy recovery.

D. Vilela, M. Guix*, J. Parmar, A. Blanco, S. Sánchez*

Micromotor-in-sponge platform for multi-cycle large-volume degradation of organic pollutants

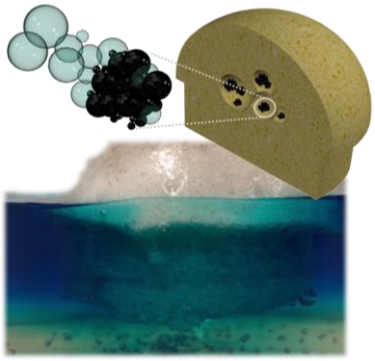

Supporting Information

Micromotor-loaded sponge for multi-cycle large-volume pollutant degradation

Diana Vilela, Maria Guix, Jemish Parmar, Àngel Blanco-Blanes, Samuel Sánchez**

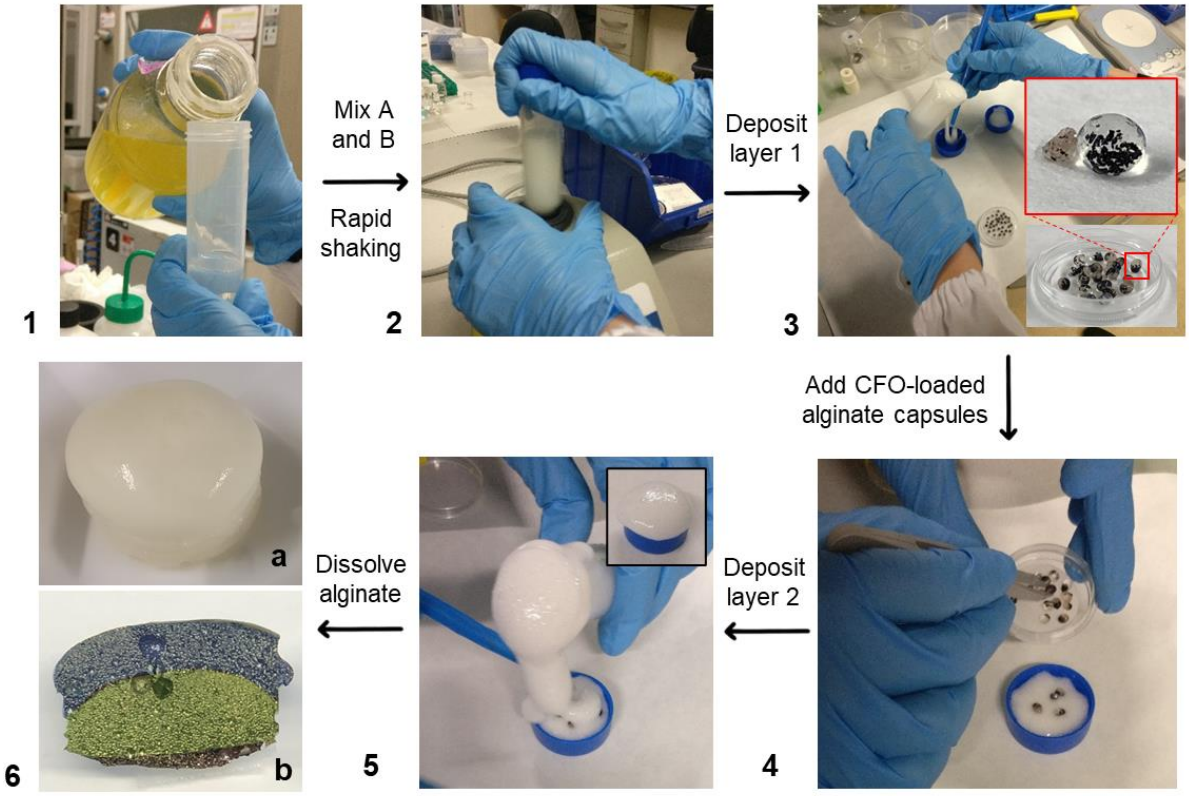

Figure S1. CFO-Sponge fabrication process.

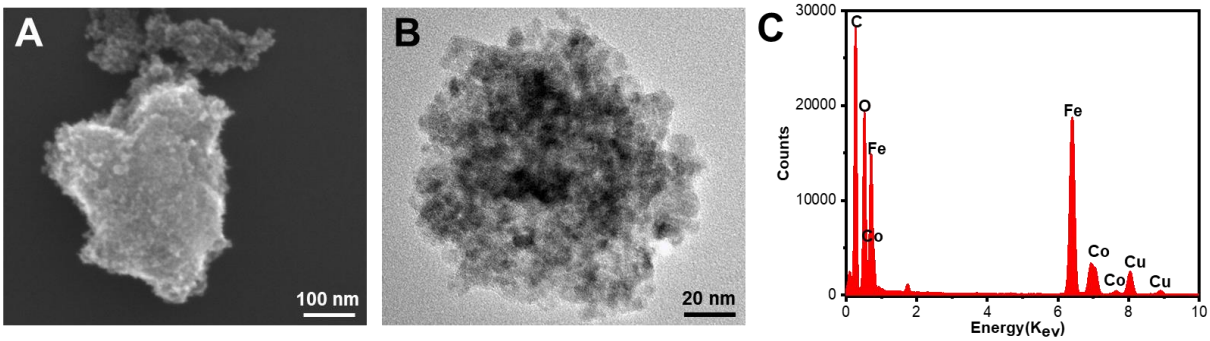

Figure S2. Characterization of CFO micromotors: (A) SEM image, (b) TEM image and (c) EDX analysis of CFO micromotors.

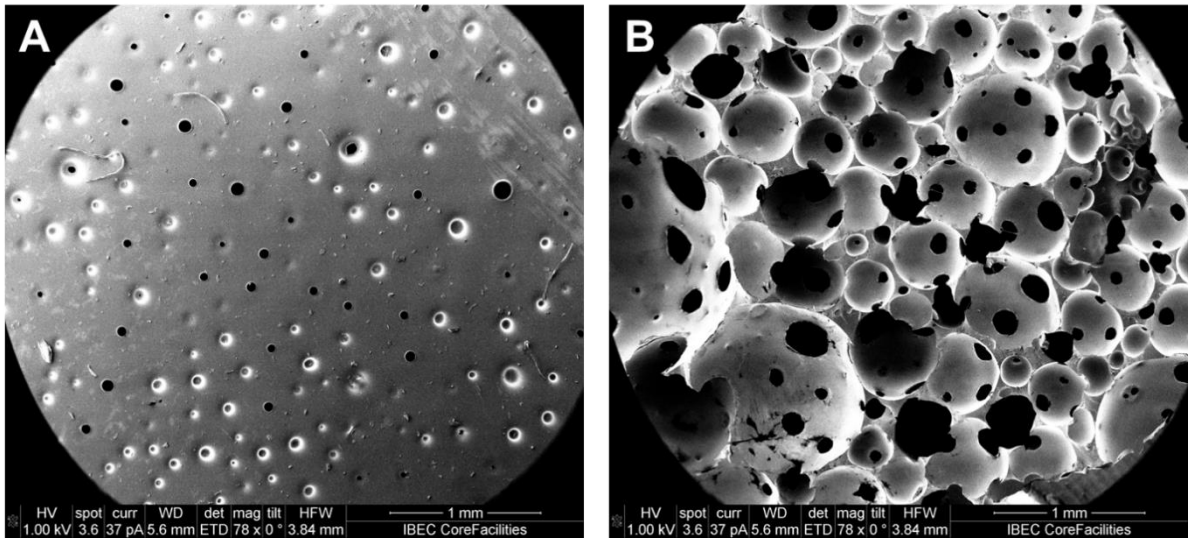

Figure S3. Sponge porosity characterization. SEM images from the smooth outer surface (A) and rough inner surface (B) of the sponge.

Movie 1. Multi-cycle pollutant degradation, depicting the two-phase system associated to the fluid flows generated during the degradation process.

Movie 2. Mixing area at the sponge-solution interface during the active degradation process promoted by the CFO micromotors embedded at the sponge core.